THE JOURNAL OF BIOLOGICAL CHEMISTRY VOL. 283, NO. 42, pp. 28115–28124, October 17, 2008

Human Follicular Fluid Heparan Sulfate Contains Abundant 3-*O*-Sulfated Chains with Anticoagulant Activity*[S]

Received for publication, July 14, 2008 Published, JBC Papers in Press, July 31, 2008, DOI 10.1074/jbc.M805338200

Ariane I. de Agostini[‡1], Ji-Cui Dong[‡], Corinne de Vantéry Arrighi[‡], Marie-Andrée Ramus[‡], Isabelle Dentand-Quadri[‡], Sébastien Thalmann[‡], Patricia Ventura[‡], Victoria Ibecheole[‡], Felicia Monge[§¶‖], Anne-Marie Fischer[§¶‖], Sassan HajMohammadi[**], Nicholas W. Shworak[**], Lijuan Zhang[‡‡], Zhenqing Zhang[§§], and Robert J. Linhardt[§§]

From the [‡]Department of Gynaecology and Obstetrics, Geneva University Hospitals and University of Geneva, Geneva 14, Switzerland, [§]Université Paris Descartes, Faculté of Médecine, Paris, F-75014, France, [¶]INSERM Unité 765, Paris, F-75006, France, [‖]Assistance Publique-Hôpitaux de Paris, Service d'Hématologie Biologique, Hôpital Européen Georges Pompidou, Paris, F-75015, France, [**]Section of Cardiology, Department of Medicine, Dartmouth Medical School, Hanover, New Hampshire 03756, the [‡‡]Department of Pathology and Immunology, Washington University School of Medicine, St. Louis, Missouri 63110, and the [§§]Department of Chemistry and Chemical Biology, Center for Biotechnology and Interdisciplinary Studies, Rensselaer Polytechnic Institute, Troy, New York 12180

Anticoagulant heparan sulfate proteoglycans bind and activate antithrombin by virtue of a specific 3-*O*-sulfated pentasaccharide. They not only occur in the vascular wall but also in extravascular tissues, such as the ovary, where their functions remain unknown. The rupture of the ovarian follicle at ovulation is one of the most striking examples of tissue remodeling in adult mammals. It involves tightly controlled inflammation, proteolysis, and fibrin deposition. We hypothesized that ovarian heparan sulfates may modulate these processes through interactions with effector proteins. Our previous work has shown that anticoagulant heparan sulfates are synthesized by rodent ovarian granulosa cells, and we now have set out to characterize heparan sulfates from human follicular fluid. Here we report the first anticoagulant heparan sulfate purified from a natural human extravascular source. Heparan sulfate chains were fractionated according to their affinity for antithrombin, and their structure was analyzed by ^{1}H NMR and MS/MS. We find that human follicular fluid is a rich source of anticoagulant heparan sulfate, comprising 50.4% of total heparan sulfate. These antithrombin-binding chains contain more than 6% 3-*O*-sulfated glucosamine residues, convey an anticoagulant activity of 2.5 IU/ml to human follicular fluid, and have an anti-Factor Xa specific activity of 167 IU/mg. The heparan sulfate chains that do not bind antithrombin surprisingly exhibit an extremely high content in 3-*O*-sulfated glucosamine residues, which suggest that they may exhibit biological activities through interactions with other proteins.

Follicular fluid contains components of the coagulation cascade and subsequent to ovulation undergoes clotting within the ruptured follicle. Yet the timing of this process must be tightly regulated as a liquid state must initially be maintained for the oocyte to be successfully delivered to the oviduct. Given the complexity of coagulation, there are likely multiple mechanisms to regulate clotting of follicular fluid. One such mechanism could involve heparan sulfate proteoglycans (HSPGs).[2]

HSPGs are ubiquitously distributed on the surface of animal cells and are secreted into the extracellular environment. They have numerous important biological activities mediated through interactions with diverse proteins. HSPGs are composed of a core protein with covalently attached HS chains formed by repetitive sulfated disaccharides of uronic acid and glucosamine. The different length and variable sequence of sulfated disaccharides generate the structural diversity required to form specific oligosaccharide-binding sites for proteins such as growth factors, protease inhibitors, or cell adhesion molecules. The reactivity of proteins is affected by their binding to HS. This principle is exemplified by heparin and anticoagulant HS (aHS), which bind to antithrombin (AT) and thereby accelerate the rate at which AT inhibits serine proteases in the blood-clotting cascade.

The AT-binding pentasaccharide of heparin and aHS proteoglycans (aHSPGs) is the best characterized biologically active structure of HS. It specifically binds and activates AT by inducing a conformational change in the inhibitor that stabilizes its active conformer. This pentasaccharide bears a 3-*O*-sulfated glucosamine essential for AT binding (1, 2). These 3-*O*-sulfates are added late in the biosynthetic pathway of HS by 3-*O*-sulfotransferases (3-OSTs). Seven isoforms of 3-OSTs

* This work was supported, in whole or in part, by National Institutes of Health Grant GM38060 (to R. J. L.). This work was also supported by Swiss National Foundation Grant 3200B0-102148/1 (to A. d. A.). The costs of publication of this article were defrayed in part by the payment of page charges. This article must therefore be hereby marked "*advertisement*" in accordance with 18 U.S.C. Section 1734 solely to indicate this fact.

[S] The on-line version of this article (available at http://www.jbc.org) contains supplemental Figs. 1 and 2 and Tables 1–3.

[1] To whom correspondence should be addressed: Fondation pour Recherches Médicales, 1205 Genève, Switzerland. Fax: 41-22-347-5979; E-mail: Ariane.Deagostini@medecine.unige.ch.

[2] The abbreviations used are: HSPG, heparan sulfate proteoglycan; HS, heparan sulfate; aHS, anticoagulant HS; iHS, anticoagulantly inactive HS; hFF, human follicular fluid; GAG, glycosaminoglycan; GC, granulosa cell; PG, proteoglycan; FSH, follicle stimulating hormone; CHAPS, 3-[(3-cholamidopropyl)dimethylammonio]-1-propanesulfonate; IdoUA2S, 2-*O*-sulfated iduronic acid; ΔUA-GlcNAc, nonsulfated disaccharides; ΔUA-GlcNS, *N*-sulfated disaccharides; ΔUA-GlcNAc6S, 6-*O*-sulfated disaccharides; ΔUA-GlcNS6S, *N*-,6-*O*-di-sulfated disaccharides; TIC, total ion chromatogram; aPTT, activated partial thromboplastin time; PT, prothrombin time; TT, thrombin time; FSH, follicle-stimulating hormone; PBS, phosphate-buffered saline; HPLC, high pressure liquid chromatography; IVF, *in vitro* fertilization; LC, liquid chromatography; MS, mass spectrometry; MS/MS, tandem mass spectrometry; RT, reverse transcription; AT, antithrombin; 3-OST, 3-*O*-sulfotransferase; MOPS, 4-morpholinepropanesulfonic acid.

have been identified, with different tissue expression patterns and acceptor substrate specificities. The 3-*O*-sulfotransferase-1 (3-OST-1) is expressed in many tissues with a particularly high expression in endothelial cells. It is the predominant isoform that produces AT-binding pentasaccharides in aHS (3), whereas other forms, such as 3-OST-3, introduce 3-*O*-sulfates in HS chains to predominantly produce structures with a distinct biologic activity (4–6). The 3-OST-5 can also generate aHS, but its expression pattern is extremely limited (4, 7).

In addition to AT, 3-*O*-sulfated HS also displays functional interactions with a viral envelope protein mediating the binding and entry into cells of herpes simplex virus 1 (5). Moreover, the coreceptor activity of HS for FGF-7 interaction with its epithelial cell receptor FGFR2IIIb is because of aHS chains containing the canonical 3-*O*-sulfated AT-binding pentasaccharide (8). These data suggest that aHSPG might have additional coreceptor activities toward certain protein ligands such as cytokines.

The aHSPGs are produced by endothelial cells and are thought to endow the vascular wall with antithrombotic properties, but they are also abundant in the reproductive tract. In the ovary, aHSPGs are strongly expressed in granulosa cells of preovulatory follicles where they are colocalized with serine protease inhibitors involved in the control of proteolytic activities at ovulation. In extravascular compartments, aHSPGs are thought to contribute to the control of proteolysis and inflammation during tissue remodeling (9–11).

Soluble forms of aHSPGs have been observed in cultured rat granulosa cells (GCs) and in rat follicular fluid, suggesting that aHSPG might be released with follicular fluid at ovulation to maintain its liquid state (12). Indeed, human follicular fluid (hFF) contains the secretions of ovarian follicular GCs.

We now report detection of a strong signal for soluble aHSPG in hFF collected from follicles of women undergoing oocyte pickup for *in vitro* fertilization (IVF) treatments, using the ^{125}I-AT ligand binding assay developed in our laboratory (13). We have purified and characterized hFF 3-*O*-sulfated aHS and show it is endowed with exceptionally potent anticoagulant activity. The presence of such a powerful anticoagulant suggests soluble aHSPGs in hFF may well serve to delay postovulatory clotting. We additionally find that hFF contains abundant 3-*O*-sulfated HS devoid of AT affinity that are anticoagulantly inactive (iHS). Given the functional diversity of HS, iHSPGs of hFF might play a role distally from the ovary, in the oviduct at fertilization or in the uterus at implantation.

EXPERIMENTAL PROCEDURES

Materials

Purified human AT was obtained from Talecris Biotherapeutics, Research Triangle Park, NC. Porcine mucosal heparin was from Diosynth Inc., Chicago IL, or as soluble anticoagulant Liquemin (Hoffmann-La Roche). Chondroitin sulfate A (from Sigma) and heparin have a $M_{r(av)}$ of 21,600 and 16,400, respectively (12). An HS standard with an $M_{r(av)}$ of 15,500 was kindly provided by C. van Gorp (Celsus Laboratories, Inc.). All other chemicals used were of the highest grade available.

Collection of hFF and Human Granulosa Cells

Follicular Fluid— hFF was collected from patients attending the Unité de Médecine de la Reproduction at Geneva University Hospital and scheduled for IVF treatment of infertility with gonadotrophin-induced ovulation. Informed consent was obtained according to a protocol approved by the local ethics committee, and follicular fluid was recovered at the time of oocyte pickup, after removal of the oocytes for IVF.

The hFF samples were pooled for each patient, carefully avoiding samples containing washing solution (gentamycin-supplemented MOPS containing 2.5 IU/ml Liquemin), and cleared by centrifugation, at low speed to remove cells (800 × *g*, 10 min, 20 °C) and subsequently at high speed to remove insoluble aggregates (13,000 × *g*, 30 min, 4 °C). The first low speed centrifugation allowed the recovery of human GCs. The supernatant was called native hFF and used in the experiments described.

For clotting assays, hFF samples were quickly taken from the hFF pool before centrifugation and supplemented with 1/10 volume of sodium citrate (0.13 M), to prevent spontaneous activation of coagulation. Citrated samples were purified by centrifugation as for the rest of the hFF pool. Blood contamination was evaluated by counting the red blood cells, and only hFF samples with blood contamination below 1% were used for coagulation tests. Samples were stored at −80 °C in aliquots until used.

Anticoagulant Activity—The prothrombin time (PT) and the activated partial thromboplastin time (aPTT) measure the activation of the extrinsic and intrinsic pathway of the coagulation cascade, respectively, and are sensitive to decreased levels of coagulation factors. The thrombin time (TT) measures the inactivation rate of thrombin, and the anti-Factor Xa activity measures the ability of HS/heparin to enhance AT inhibition of this coagulation protease. aPTT and TT are prolonged in the presence of unfractionated heparin.

These and additional hemostatic assays were used to analyze hFF as well as aHS and iHS purified from hFF. Native hFF was supplemented with 1/10 volume of 0.13 M sodium citrate, and purified aHS and iHS were resuspended in 0.15 M NaCl.

All measurements, except D-dimers, were made on Diagnostica Stago Analyzer (STA-R). Measurements were made using Automated aPTT from Bio-Merieux (Durham, NC), human thrombin from Sigma for TT, and STA Neoplastine CI 10 from Diagnostica Stago (Asniere, France) for PT; Diagnostica Stago STA deficient II, STA deficient V, or STA deficient VII were used for Factor II, Factor V, and Factor VII levels, respectively. Fibrinogen S (Diagonostica Stago) was used for fibrinogen level, Stachrom AT III (Diagnostica Stago), for chromogenic AT assay. STA Rotachrom heparin (Diagnostica Stago) was used for chromogenic heparin activity anti-Factor Xa assay with a standard curve done with unfractionated heparin. D-dimers were measured using a kit D-DI Test® (Diagnostica Stago). Assays were performed according to the manufacturer, or with the modifications described below. Dilutions were done using Owren-Koller buffer.

Due to a small amount of hFF available, different coagulation parameters previously tested by others (14, 15) were measured

only on three different samples, one sample being extensively tested to explore the PT prolongation. Reagents used to perform the PT contain a polycation that neutralizes negatively charged GAGs, such as heparin, up to 1 unit/ml heparin. To determine whether the PT decrease was because of the presence of a high amount of HS or to decreased levels of coagulation factors, the PT was compared in native hFF serially diluted either in buffer or in normal plasma containing coagulation factors. Similarly, anti-Factor Xa levels were tested in parallel in hFF diluted in normal plasma and in buffer with AT. Anti-Factor Xa level was measured in citrated native hFF from 12 individual patients diluted (1:2 to 1:16) in normal plasma.

Detection of aHSPG in hFF by ^{125}I-AT-ligand Binding Assay—The presence of aHSPG was detected by ^{125}I-AT-binding as described previously (13). Briefly, native hFF was filtered on a 0.22-μm Millex filter to remove insoluble material and loaded on a nitrocellulose membrane using a dot-blot apparatus. The amount of protein loaded per well was kept below 20 μg to avoid saturation of the membrane, which was subsequently saturated in blotto buffer (5% nonfat dry milk in 10 mM Tris-HCl, pH 7.4, 150 mM NaCl) for 30 min at room temperature and incubated for 2 h in the same buffer containing ^{125}I-AT (1×10^6 cpm/ml, ~1 nM). After five washes in the same buffer, the membrane was exposed for autoradiography, and radioactivity was quantified in a γ-counter. Measurements were done in triplicate, and the results were expressed as counts/min/ml of sample. For controls, we used conditioned media from the aHSPG-positive reference cell line LTA.

Purification of hFF aHS and iHS

Ion Exchange Batch Chromatography on DEAE-Sephacel—hFF was admixed with 0.6% CHAPS (w/v) and a half-volume of DEAE-Sephacel gel equilibrated in PBS (50 mM sodium phosphate at pH 7.4 with 150 mM NaCl). The slurry was rotary mixed for 3 h at 4 °C and subsequently washed on a glass filter with PBS until no more proteins eluted, as detected by Coomassie Blue staining of the effluent. The gel was successively washed with 2 gel volumes of PBS containing 0.6% CHAPS, with 10 volumes of PBS, with two gel volumes of 50 mM sodium acetate, pH 5.0, and with PBS to restore the pH to 7.4. The gel was then packed in a column and eluted with 2 column volumes of sodium phosphate (50 mM at pH 7.4) containing 2.0 M NaCl. Protein elution was followed by measuring absorbance at 280 nm and glycosaminoglycans (GAGs) by Alcian blue binding (Fluka Chemical Corp., Milwaukee, WI), using heparin as standard (16). Fractions containing proteins and GAGs were pooled, dialyzed against PBS, and concentrated on an Amicon concentrator (Amicon plastics, Houston, TX) using a PM30 membrane. Insoluble material was removed from the concentrate by filtration on a 0.22-μm pore size Millex membrane (Millipore Corp., Bedford, MA).

Ion Exchange Chromatography on Mono Q Resin—The sample was purified on a Mono Q ion exchange column (diameter 10 mm, 10 ml of gel) and eluted using a fast protein liquid chromatography system (GE Healthcare). The loading buffer was PBS, and after washing with PBS and with 2 column volumes of 50 mM sodium acetate (pH 5.0), the bound material was eluted in PBS with a linear gradient (130 ml of 0.15 to 3.0 M NaCl) at a flow rate of 2 ml/min. Elution was followed by absorbance at 280 nm for proteins, by Alcian blue assay for GAGs, and by ^{125}I-AT ligand-binding assay for aHSPGs. Pooled fractions were dialyzed and concentrated on an Amicon concentrator as described previously.

Gel Filtration Chromatography on Sepharose CL4B—The high molecular weight HSPGs were fractionated by gel filtration on Sepharose CL4B column (0.9 × 63 cm) in PBS. The inclusion volume ($K_{av} = 0$) of the column was determined using Dextran Blue (GE Healthcare), and the total volume ($K_{av} = 1$) was determined with 2 M NaCl, followed by conductivity. The elution position of GAG chains was determined relative to two heparin preparations (Diosynth heparin, cleaved from peptides by β-elimination (17), $K_{av} = 0.75$; Liquemin, $K_{av} = 0.62$). Chromatographic elution was followed by absorbance at 280 nm, for protein, by Alcian blue for hFF HS and by ^{125}I-AT ligand-binding assay for aHSPGs.

Purification of HS Chains from HSPG—HS chains were cleaved from HSPGs by β-elimination, and proteins were removed by phenol extraction and HS concentrated by ethanol precipitation (12).

Isolation of aHS by Affinity on Immobilized AT—aHS was isolated from iHS by AT affinity on concanavalin A-Sepharose, as described (12).

Characterization of hFF aHS and iHS

Affinity Coelectrophoresis—The binding of AT to hFF HS was analyzed by affinity coelectrophoresis as described (12). hFF aHS and iHS were loaded in separate transverse slots close to the cathode, each slot facing three rectangular sagittal wells in which AT was cast at concentrations of 0 (control), 30, and 500 nM. The HS samples were subjected to electrophoresis at 60 V and 200 mA for 5 h, and the gel was subsequently stained with Azure A. The migration profile was scanned, and R_F was determined using the Aida software (Raytest, Isotopenmessgeräte GmbH, Straubenhardt, Germany).

Determination of Average Molecular Weight of hFF aHS and iHS—Pure aHS and iHS were run on nondenaturing PAGE to estimate their molecular weight as described (12). Briefly, aHS and iHS were subjected to electrophoresis on polyacrylamide gradient (11–22%) gels without SDS, in buffer containing 0.1 M NaCl and stained using Azure A. GAG molecular weight standards were heparin ($M_{r(av)}$ 16,400), chondroitin sulfate A ($M_{r(av)}$ 21,600) and HS I ($M_{r(av)}$ 15,500). HS or standard GAG sample (5 μg) was loaded in each lane, and migration profiles were scanned and analyzed using the Aida software (Raytest, Isotopenmessgeräte GmbH, Straubenhardt, Germany). hFF HS molecular weight was determined by extrapolation from the regression of the standard GAG modal R_F and log M_r (log M_r = −27,821 R_F +33,969).

One-dimensional ^{1}H NMR Analysis—^{1}H NMR was performed on Bruker 800 spectrometer with Topsin 2.0 software. Commercial HS (from porcine intestine, Celsus Co.), aHS, and iHS (200 μg) were each dissolved in 0.5 ml of ^2H_2O (99.996%, Sigma) and freeze-dried repeatedly to remove the exchangeable protons. The samples were redissolved in 0.3 ml of ^2H_2O and transferred to an NMR Shigemi tube (Sigma). The operation conditions for spectra were as follows: frequency, 800 MHz;

TABLE 1

Coagulation parameters of three individual hFF samples

Fibrinogen reference concentration for normal plasma is 2.9 g/liter. TT reference time is 20 ± 5 s, and aPTT reference time is 35 ± 6 s.

Sample no.	PT	aPTT	Fibrinogen	TT	Anti-Factor Xa activity	D-dimers	Factor II	Factor V	Factor VII
	%	*s*	*g/liter*	*s*	*IU/ml*	*mg/ml*	*%*	*%*	*%*
1	7	>120	0.37	>60	2.1	<1	67	4.0	48
2	16	>120	0.83	>60	3	<1	69	10.0	69
3	19	>120	0.72	>60	2	<1	84	7.0	55

wobble sweep width, 20 MHz; filter width, 125 kHz; pre-scan delay, 6 μs; transmitter frequency offset, 4.704 ppm; temperature, 300 K. The water resonance was suppressed by selective irradiation during the relaxation delay.

LC-MS and MS/MS Analysis of hFF aHS and iHS Digested by Heparin Lyases—The aHS and iHS samples (30 μg, respectively) were incubated in 10 μl of 50 mM sodium phosphate buffer, pH 7.0, with heparin lyase I, II, and III (10 milliunits; Sigma) at 37 °C for 10 h. The products were heated in a boiling water bath for 10 min to halt the reaction. The denatured protein was removed by centrifugation at 12,000 × *g* for 10 min. LC-MS analyses were performed on Agilent 1100 LC/MSD instrument (Agilent Technologies, Inc. Wilmington, DE) equipped with an ion trap, binary pump, and a UV detector. The column was a 5-μm Agilent Zorbax SB-C18 (0.5 × 250 mm). Eluent A was water/acetonitrile (85:15), v/v, and eluent B was water/acetonitrile (35:65) v/v. Both eluents contained 12 mM tributylamine and 38 mM NH_4OAc, and their pH was adjusted to 6.5 with HOAc. The reaction mixtures of aHS and iHS (5 μl, respectively) were injected by autosampler. A gradient of 0% B for 15 min and 0–50% B for over 45 min was used at a flow rate of 10 μl/min. Mass spectra were obtained using an Agilent 1100 Series Classic G2445D LC/MSD trap. The electrospray interface was set in negative ionization mode with the skimmer potential of −40.0 V, capillary exit of −20.0 V, and a source temperature of 325 °C to obtain maximum abundance of the ions in a full scan spectra (150–1500 Da, 10 full scans/s). Nitrogen was used as a drying (5 liters/min) and nebulizing gas (20 p.s.i.). Auto MS/MS was turned on in these experiments using an estimated cycle time of 0.07 min. Total ion chromatograms (TIC) and mass spectra were processed using Data Analysis 2.0 (Bruker software).

Human Granulosa Cells, Culture Conditions and Detection of Cell-bound and Soluble aHSPG—Human granulosa cells were recovered from the pellet of the first centrifugation of hFF, purified by two steps of centrifugation on a 50% Percoll gradient, and cultured 2–8 days in a 1:1 mixture of F-12 and Dulbecco's modified Eagle's medium high glucose media containing 10% fetal calf serum and 1% glutamine in the presence of 50 ng/ml follicle-stimulating hormone (FSH). During the last 24 h of culture, cells in triplicate wells were kept in serum-free medium supplemented with 100 μg/ml bovine serum albumin to prepare conditioned medium, which was used for measuring soluble aHSPG by ^{125}I-AT ligand-binding assay (13). Subsequently, cell surface aHSPG were measured by ^{125}I-AT cell-binding assay (19). Estradiol was measured in granulosa cell media by radioimmunoassay as described (18).

Human GC, RT-PCR Analysis of the Expression of HS-3-O-Sulfotransferase Isoforms—Human GC, recovered from the pellet of the first centrifugation of hFF, were purified by two steps of centrifugation on a 50% Percoll cushion, and then total RNA was isolated using the TRIzol reagent according to the manufacturer's instructions (Invitrogen). Levels of 3-OST transcripts were quantified by real time RT-PCR using gene-specific first strand synthesis (19). In brief, first strand synthesis was performed using a ThermoScript RT-PCR kit (Invitrogen catalog number 11146-024) with the following modifications. Reverse transcription was performed on 300 ng of RNA in 34-μl reactions supplemented with 6.8 μg of glycogen and 10 nM of each 3-OST isoform-specific primer. Reactions lacking (RT−) or containing (RT+) 25.5 units of reverse transcriptase were incubated at 55 °C for 2 h and then RNase-treated. SYBR Green (Applied Biosystems)-based real time PCR was performed on 30-μl reactions containing cDNA derived from 10-ng eq of RNA and appropriate 3-OST isoform-specific primers. Additional reactions contained varying levels of quantitation standards, cloned PCR products for each respective 3-OST isoform. Transcripts per reaction were then determined with the GeneAmp5700 sequence detection system under standard cycling conditions. Correction for contaminating genomic DNA was accomplished by subtracting the RT− value from the RT+ value. Sequences for human 3-OST isoform-specific RT primers and PCR primers were described previously (20). Our analysis included the final family member, 3-OST-6, which was identified in a characterization of chromosome 16 by the Human Genome Project and initially referred to as 3-OST-5 (21). The results were expressed as 3-OST mRNA copies per 10 ng of total RNA.

RESULTS

hFF Contains a Potent Anticoagulant Activity

To determine whether hFF contains an aHS-like activity, we first characterized the coagulation parameters of citrated hFF collected from IVF patients in which ovulation was induced with gonadotrophins. The levels in hFF of some clotting factors such as Factor V and fibrinogen were decreased in hFF to 4.0–10% and to 13–25% of their respective plasma concentrations (Table 1). These data are in keeping with previous observations (14, 15). The PT, aPTT, and TT were markedly prolonged. These prolonged times were not due to enhanced fibrinolysis, as D-dimer levels were not elevated (Table 1). Thus, hFF exhibits a strong anticoagulant state.

The prolonged PT of hFF was likely because of the decreased Factor V and fibrinogen, as the PT was normalized when hFF was diluted in plasma to complement these factors (supplemental Table 1).[3] However the reduced levels of Factor V and

[3] The PT cannot have been prolonged by a heparin/aHS-like activity, as the thromboplastin used to activate the extrinsic pathway of the coagulation cascade contains a polycation that neutralizes negatively charged GAGs.

TABLE 2
GAG lyase digestion of hFF aHSPG

Treatment	^{125}I-AT ligand binding	
	HFF	LTA cell medium
	% untreated	
Control	100.0	100.0
Heparin lyase III	8.8	29.0
Heparin lyase I	83.1	98.0
Chondroitinase ABC	98.7	98.0

fibrinogen are insufficient to explain the profound prolongation in the aPTT and TT, which suggests the presence of an inhibitor of clotting. In particular, the TT measures clot formation by exogenously added thrombin, so the extremely prolonged TT indicates the presence of a thrombin inhibitor, such as heparin/aHS. hFF contains an AT level comparable with plasma (supplemental Table 1) that would enable manifestation of a heparin/aHS-like activity.

Indeed, hFF exhibited a high anti-Factor Xa activity, which indicates a strong heparin/aHS-like anticoagulant activity (Table 1). This activity was lost when hFF was diluted in buffer but retained with dilution in plasma, which suggests the anti-Xa activity requires a plasma cofactor such as antithrombin (supplemental Table 1). With an expanded dataset of hFF from 12 individual patients, we detected remarkably similar values between individuals ranging from 1.88 to 3.52 anti-Xa units/ml (mean 2.5 + 0.5 IU/ml). This anticoagulant activity is extremely high given that the therapeutic range for heparin is 0.5–1 IU/ml.

hFF Contains Extremely High Levels of aHSPGs

The above data suggest that hFF may possess aHSPGs, so this possibility was tested with our well established ^{125}I-AT-ligand binding assay (13). hFF exhibited binding sites for ^{125}I-AT that were extremely sensitive to predigestion with heparin lyase III (which degrades HS), partially sensitive to heparin lyase I (which degrades heparin), and insensitive to chondroitinase ABC; thereby indicating that the sites reside in aHSPGs (Table 2). Surprisingly, hFF showed extraordinarily high levels of aHSPGs, with a signal of $302 \times 10^6 \pm 35 \times 10^6$ cpm/ml. This signal was about 2000-fold higher than that for conditioned medium from our "highly expressive" reference cell line, LTA ($0.15 \times 10^6 \pm 0.01 \times 10^6$ cpm/ml). Between patients, hFF levels of aHSPGs and anti-Factor Xa activity correlated extremely well ($r = 0.659$, $p < 0.02$, $n = 12$), which suggests that aHSPGs may well account for the high anti-Factor Xa activity of hFF (supplemental Fig. 1).

Purification of hFF aHS and iHS

Isolation of hFF HS—The above possibility was further explored by purifying and characterizing HS species from hFF. Initial analytical purification showing tight binding of hFF aHSPG to ion exchange resin (supplemental Fig. 2) prompted us to begin purification by a batch adsorption on DEAE-Sephacel to remove the majority of hFF proteins. The PG fraction was eluted with 2 M NaCl.

After desalting and concentration, the HSPG fraction was purified on Mono Q ion exchange resin, and the fractions positive for GAG and for aHSPG, eluting between 0.96 and 1.38 M NaCl, were pooled (Fig. 1*A*). This pool contained a minor peak of protein, whereas most of the protein eluted early in the salt gradient, at ~0.3–0.7 M NaCl. The PG fraction was dialyzed and concentrated, and non-HS GAGs (chondroitin sulfate, dermatan sulfate, and hyaluronan) were degraded with chondroitinase ABC.

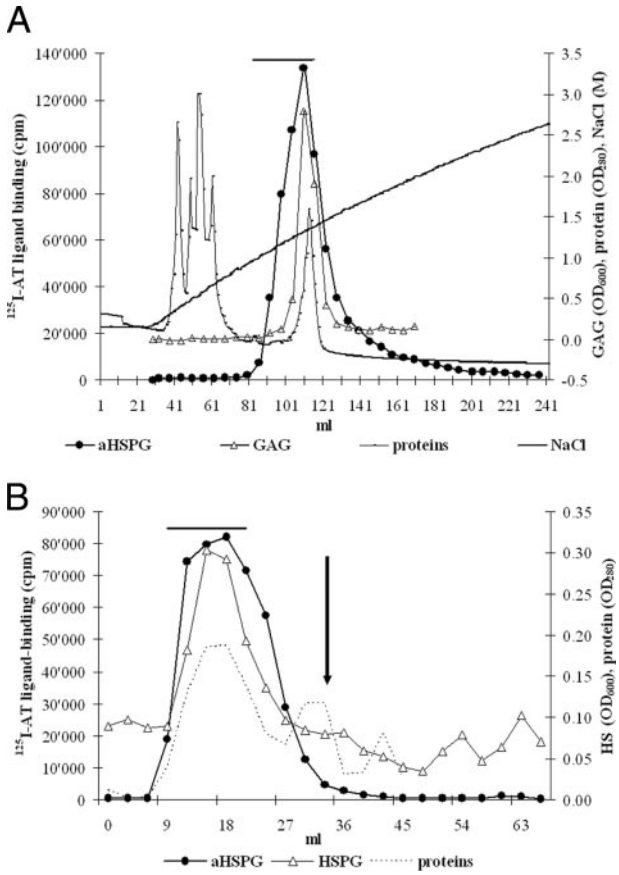

FIGURE 1. **Purification of hFF HSPG by ion exchange and gel filtration chromatography.** *A*, fractionation of hFF PG by Mono Q chromatography. The column was loaded and washed with PBS buffer containing 0.15 M NaCl and eluted by a NaCl gradient. Proteins were followed by A_{280}; the aHSPG was followed by the ^{125}I-AT ligand-binding assay and the GAG by Alcian blue. Positive fractions were detected between 0.96 and 1.76 M NaCl, and the fractions eluting between 0.96 and 1.38 M NaCl were pooled for further purification (*bar*). *B*, gel filtration of hFF HSPG on Sepharose CL4B. HSPG (followed by Alcian blue) eluted as a major high molecular weight peak containing all the aHSPG (followed by ^{125}I-AT ligand binding). Fractions eluting at K_{av} 0–0.1 were pooled for further analysis (*bar*). Minor HS peaks of lower molecular weight representing free GAG were discarded. For comparison, heparin ($M_{r(av)}$16,400) eluted at K_{av} 0.6 (*arrow*) clearly separated from the HSPG peak.

The hFF HSPGs were further purified by gel filtration on Sepharose CL4B with a major high molecular weight HSPG peak containing protein, GAG, and aHSPG, which eluted at K_{av} 0.0–0.1 and was clearly separated from free GAGs (Fig. 1*B*). The high molecular weight HSPG fractions were pooled.

HS chains were isolated from the HSPG pool by β-elimination cleavage from the PG core protein under conditions avoiding loss of sulfate groups. The HS fraction was then purified by phenol extraction and concentrated by ethanol precipitation.

Fractionation of aHS and iHS on Immobilized AT—The HS was then fractionated into aHS and iHS based on their affinity for AT. AT and HS were incubated together to allow the formation of aHS·AT complexes that were isolated from iHS by

TABLE 3
Isolation of aHS and iHS by AT affinity
Values are means ± S.E., $n = 6$.

Sample	aHS	iHS
μg of HS/ml hFF	1.8 ± 0.2	1.8 ± 0.5
% HS	50.4 ± 5.1	49.6 ± 5.1

binding of the AT moiety to concanavalin A-Sepharose. The bound aHS was eluted with 1 M NaCl, and after desalting, the iHS and aHS fractions were purified by phenol extraction and concentrated by ethanol precipitation. aHS and iHS were quantified with Alcian blue, and the yield was typically of about 100 μg of aHS and 100 μg of iHS from 60 ml of starting hFF (Table 3).

The hFF HS was found to contain 50.4% aHS, a very high proportion because AT-binding chains usually represent 5–15% of total HS and a maximum of 30% of heparin chains. In terms of recovery, 60 ml of native hFF contained 15.66 ± 1.67 mg of total GAG, most of which was contributed by hyaluronan, chondroitin, and dermatan sulfates (22–25). We recovered 0.39 ± 0.06 mg of HS chains after β-elimination, which represents 2.5% of the starting GAG. The yield for the affinity fractionation into aHS and iHS was 55.3%, with losses being mainly because of low amounts of material (supplemental Table 2). The purification showed remarkably stable yields in HS (supplemental Table 2), reflecting the fine-tuning of the superovulation induced in the IVF patients by FSH treatment.

Characterization of aHS and iHS

The purified hFF aHS and iHS were characterized by determining their anticoagulant activity, AT affinity, molecular weight, 3-*O*-sulfate content, and their structure by one-dimensional ^{1}H NMR, as well as by LC-MS and MS/MS.

Anticoagulant Activity of Purified aHS and iHS—We have analyzed the anti-Factor Xa activity of pure aHS and iHS and determined their specific anticoagulant activity. The iHS fraction, which did not bind AT during the purification, exhibited undetectable anti-Factor Xa activity, even at the highest concentration tested of 200 μg/ml. In contrast, aHS had a very high anticoagulant activity of 167 ± 22 IU/mg. This value is comparable with that of standard unfractionated heparin (133 IU/mg) and is the highest specific anticoagulant activity reported for HS. As little as 1.5 μg/ml of hFF aHS was sufficient to prolong the aPTT (47 s *versus* reference value of 32 ± 6 s) and thrombin time (26 s *versus* reference value of 19 ± 5 s) of plasma. Taken together, these results demonstrate that hFF aHS has a potent anticoagulant activity mediated by AT, with a specific anti-Factor Xa activity similar to that of heparin.

Given that aHS has a specific activity of 167 IU/mg, we have calculated that the anti-Factor Xa activity measured in native hFF (2.5 IU/ml) corresponds to 16.7 μg/ml aHS. Thus, the purification yield of hFF aHS was of 10.7%. Because aHS represents 50.4% of the total HS, hFF contains about 33.2 μg/ml of total HS.

Coelectrophoresis Analysis of the AT Affinity of hFF aHS and iHS—AT affinity was analyzed semi-quantitatively by affinity coelectrophoresis. Pure hFF aHS and iHS were loaded on an agarose gel containing various amounts of AT cast in the gel.

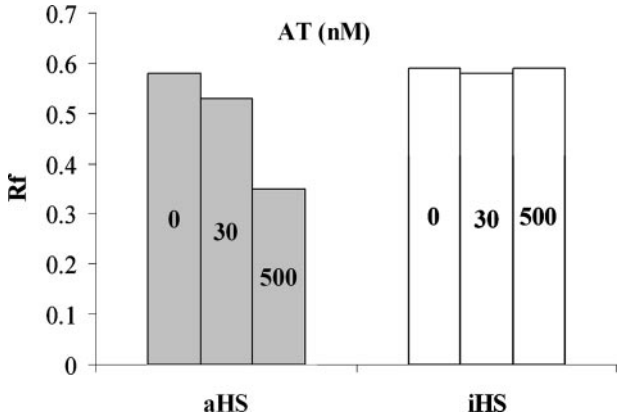

FIGURE 2. **aHS·AT complexes have retarded migration on affinity coelectrophoresis.** The hFF aHS and iHS (10 μg/lane) were subjected to electrophoresis in an agarose gel containing the indicated concentrations of AT. Densitometry scanning of the Azure A-stained gel shows that aHS is retarded in the presence of 30 nM AT and further retarded with 500 nM AT. In contrast, iHS migration is not affected by the presence of AT. The figure shows the data for one representative experiment. Similar results were obtained in three independent experiments.

The formation of aHS·AT complexes retards the migration of aHS. aHS migration was retarded with 30 and 500 nM AT, but iHS migration was unretarded at all AT concentrations (Fig. 2). These data are comparable with those obtained for aHS from cultured rat microvascular endothelial and granulosa cells (12), suggesting that hFF aHS binds to AT with an affinity similar to aHS from endothelial cells.

HS Chain Size—The molecular weight of hFF aHS and iHS was determined by PAGE using calibrated molecular weight standards. Fig. 3 shows that hFF aHS and iHS exhibited a moderately smeared migration profile, as expected from the polydispersity of HS. The size distribution was similar for aHS and iHS, and the modal M_r was 28,750 ± 1,750, and 31,000 ± 6,140, respectively (for two independent preparations). The slightly lower chain size of aHS is likely artifactual because aHS has a greater sulfate content than iHS (as indicated below), which would enhance electrophoretic migration. Thus, aHS and iHS exhibit a modal M_r of about 30,000 Da.[4]

HS One-dimensional ^{1}H NMR Spectra and 3-O-Sulfate Content—One-dimensional ^{1}H NMR spectroscopy (Fig. 4) revealed that compared with a commercial HS standard, hFF aHS and iHS exhibit a lower content of residues containing 2-*O*-sulfated iduronic acid (IdoUA2S), iduronic acid, and 6-*O*-sulfated glucosamine (GlcNAc) (*peaks b, c, d, f,* and *g*) and conversely contain a higher content of nonsulfated GlcNAc

[4] The susceptibility of hFF aHS and iHS to digestion was tested using heparin lyases I and III, which degrade highly sulfated (heparin like) and poorly sulfated disaccharides, respectively. Both aHS and iHS chains were minimally degraded by heparin lyase I treatment and were more sensitive to heparin lyase III, whereas simultaneous digestion by heparin lyase I and III produced small fragments resistant to digestion (data not shown). These data suggest that aHS and iHS chains have similar low sulfated domains interspersed with restricted highly sulfated domains. Fragments resistant to digestion with both heparin lyases I and III might contain 3-*O*-sulfated residues, which are resistant to the action of heparin lyases (26, 27). Given its high level of AT-binding sites, aHS was expected to have a high level of 3-*O*-sulfated residues. Conversely, a high content of 3-*O*-sulfates in iHS that lacks AT-binding sites was surprising and prompted us to further explore the composition of aHS and iHS by one-dimensional ^{1}H NMR analysis.

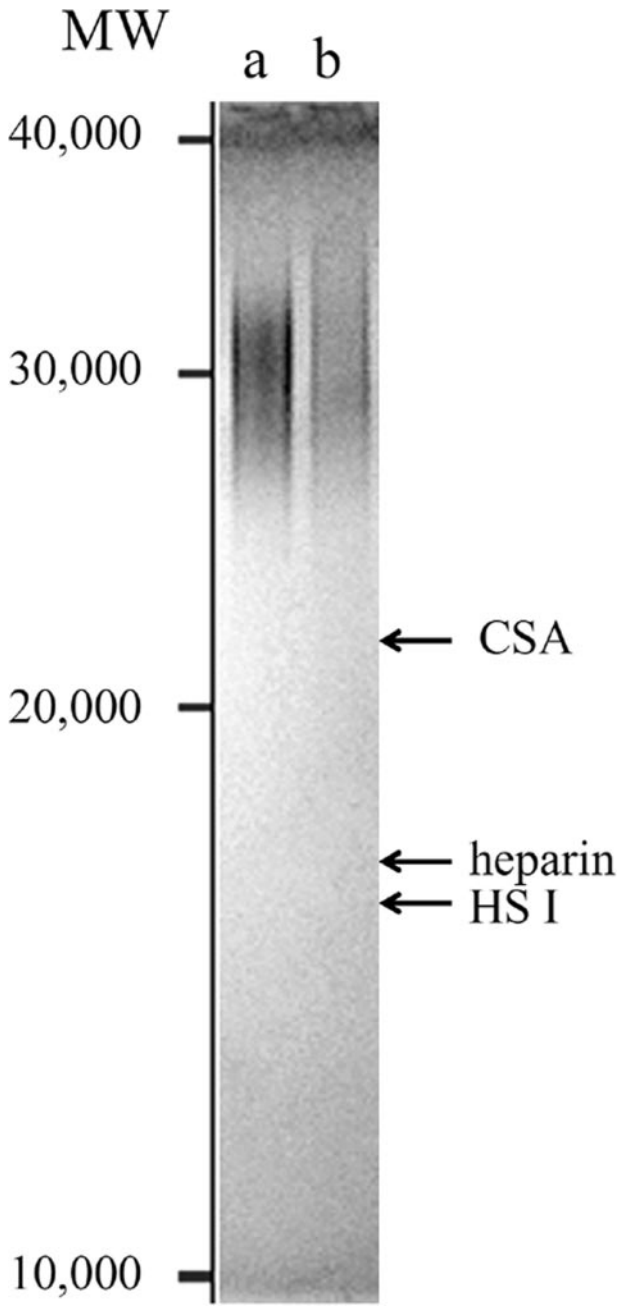

FIGURE 3. **Molecular size distribution of hFF aHS and iHS.** A representative example of molecular weight determination for aHS (*a*) and iHS (*b*). Azure A-stained PAGE shows similar size distribution of aHS and iHS. The migration position of standard GAG is indicated by *arrows*, heparin ($M_{r(av)}$16,400), chondroitin sulfate A ($M_{r(av)}$ 21,600), and HS I ($M_{r(av)}$15,500). The modal molecular mass of aHS and iHS is about 30,000 Da.

(H-4,5,6; Fig. 4, *peak i*). Moreover, peak i (H-4,5,6 of GlcNAc) was higher in iHS than aHS. Combined, these data reveal the degree of sulfation follows the order of HS standard > aHS > iHS.

The signal for 3-*O*-sulfated glucosamine residues (Fig. 4, *peak e′*; H-3 of 3-*O*-sulfated glucosamine or *N*-,6-*O*-di-sulfated glucosamine) partially overlaps with peak e. Peak e′ for aHS is readily detected by spectral subtraction (aHS minus iHS). Thus, hFF aHS, compared with iHS, contains a greater level of 3-*O*-sulfated glucosamine residues.

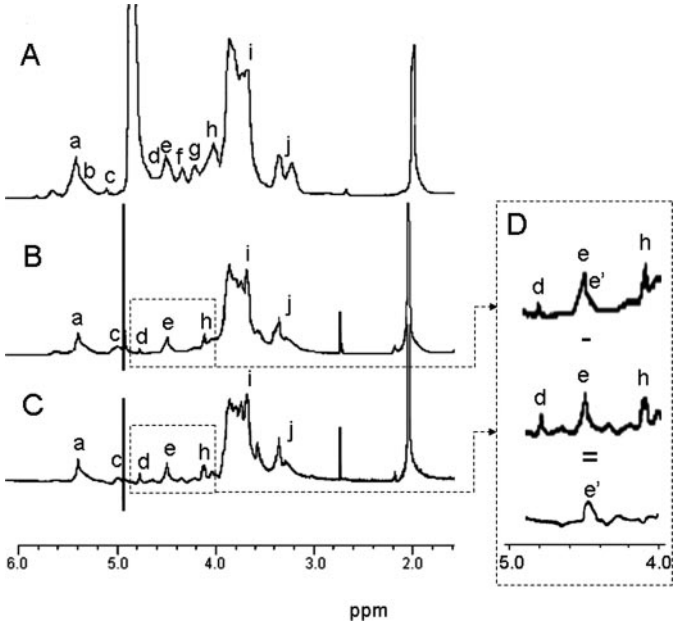

FIGURE 4. **^{1}H NMR spectra of standard HS and hFF derived aHS and iHS.** Shown are ^{1}H NMR spectra of a commercial HS standard (*A*), hFF aHS (*B*), and hFF iHS (*C*). The presence of H-3 of GlcNS3S and GlcNS3S6S (*peak e′*) in *B* is highlighted in *D* by expanding the indicated spectral regions and by showing the difference spectrum of *B* minus *C*. *Peak a*, H-1 GlcNAc; *peak b*, H-1 IdoUA2S; *peak c*, H-1 IdoUA; *peak d*, H-5 IdoUA2S; *peak e*, H-1 GlcA; *peak f*, H-2 IdoUA2S; *peak g*, H-3 IdoUA2S; *peak h*, H-6 GlcNS6S or GlcNAc6S; *peak i*, H-4,5,6 GlcNAc; *peak j*, H-2 GlcNS.

LC-MS and MS/MS Analysis of the Saccharide Composition of hFF aHS and iHS—To further characterize the chemical structure of hFF aHS and iHS, we performed capillary HPLC-MS of samples extensively digested by heparin lyase I, II, and III (Fig. 5). Digests of aHS and iHS contained four disaccharides ((Fig. 5, *peaks 1–4*) and five digestion-resistant tetra- and hexasaccharides (*peaks 4–8*). The compositional analysis (Fig. 5*C*) indicates that aHS and iHS, respectively, contain 1.21 and 1.09 sulfate groups per disaccharide, and so confirm the one-dimensional ^{1}H NMR finding that aHS is more heavily sulfated than iHS. MS/MS analyses revealed the structure of the tetrasaccharides (Fig. 6) and demonstrated that peak 8 contained two components.

The first component (Fig. 6, *peak 8-1*) was a 3-*O*-sulfated tetrasaccharide (ΔUA2S-GlcNAc-UA-GlcNS6S3S) that was more abundant in aHS than iHS (11.2 *versus* 9%; Fig. 5). Based on an average chain size of 30,000 Da, aHS and iHS both contain about five 3-*O*-sulfate substituents derived from this tetrasaccharide. Thus, these data reveal that both aHS and iHS contain abundant 3-*O*-sulfated glucosamine residues.

The second component (Fig. 5*C*, *peak 8-2*) was a hexasaccharide (ΔUA-GlcNAc-UA-GlcNS-UA-GlcNS + 2S) that was 10-fold more abundant in aHS than in iHS digests (Fig. 5*C*). Indeed, the difference in levels of this sulfate-rich hexasaccharide accounts for aHS being more heavily sulfated than iHS. It was not possible to assign locations for two of the sulfate groups; however, the resistance of this hexasaccharide to heparin lyase digestion suggests that it contains at least one 3-*O*-sulfated glucosamine residue (26, 27). Such a composition would account for the one-dimensional ^{1}H NMR data showing

that aHS, compared with iHS, contains a greater level of 3-*O*-sulfated glucosamine residues.

Human Ovarian GCs Synthesize aHSPG

hFF Contains aHSPG Synthesized by Human GC—We next tested if hFF aHSPGs are derived from GCs by employing ^{125}I-AT-ligand binding to analyze cultured human primary GCs. We detected both cell-bound and soluble aHSPGs from cultured human GCs in amounts comparable with those seen in the aHSPG-positive fibroblastic cell line LTA (Fig. 7*A*) and in rat GCs (12). Cultured human GCs secreted estradiol, and we found a strong correlation between the amount of estradiol secreted and of aHSPG on the cells (Fig. 7*A*). This correlation suggests that FSH up-regulates aHSPG synthesis.

Human Granulosa Cell Expression of 3-O-Sulfotransferases—Given the unusually high anticoagulant activity of hFF HS, we sought to determine which 3-OST isoforms may be responsible for hFF aHS synthesis. Consequently, we used quantitative RT-PCR to measure the transcript levels of all seven isoforms of 3-OST in human primary GCs (Fig. 7*B*). RNA was extracted from cells after isolation by Percoll density gradient centrifugation.

The results show that multiple isoforms of 3-OST are expressed by human GCs isolated 35 h after ovulation induction. The 3-OST-1 isoform was strongly predominant, with an expression level almost 100-fold higher than 3-OST-3A and 3-OST-5 and 1000-fold higher than 3-OST3B.

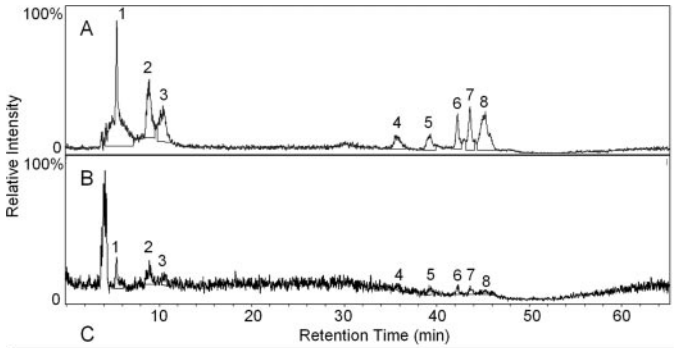

Peak No.	Mass (m/z)	Structure	Content in aHS	Content in iHS
1	378.1	ΔUA-GlcNAc	23.3%	27.2%
2	416.1	ΔUA-GlcNS	14.0%	22.5%
3	458.1	ΔUA-GlcNAc6S	11.9%	10.7%
4	496.1	ΔUA-GlcNS6S	4.9%	5.5%
5	437.1	ΔUA2S-GlcNS-UA-GlcNAc	4.9%	9.4%
6	456.1	ΔUA-GlcNS-UA-GlcNS6S	5.4%	6.5%
7	477.1	ΔUA2S-GlcNAc-UA-GlcNS6S	8.1%	7.5%
8-1	517.1	ΔUA2S-GlcNAc-UA-GlcNS6S3S	11.2%	9.0%
8-2	685.1	ΔUA-GlcNAc-UA-GlcNS-UA-GlcNS +2S	16.3%	1.6%

FIGURE 5. **TIC and oligosaccharide composition of hFF aHS and iHS following enzymatic digestion.** *A*, TIC of hFF aHS; *B*, TIC of hFF iHS; *C*, composition table of each fraction. MS and MS/MS analyses confirmed the structures of the indicate disaccharides (data not shown) and oligosaccharides (Fig. 6).

DISCUSSION

The coagulation status of follicular fluid is regulated relative to the female reproductive cycle. An anticoagulant state initially exists during follicle growth (the follicular phase) and rupture (the ovulatory phase). Prevention of clotting after ovulation ensures that follicular fluid can serve as a conduit for delivery of the oocyte to the oviduct. In contrast, during the

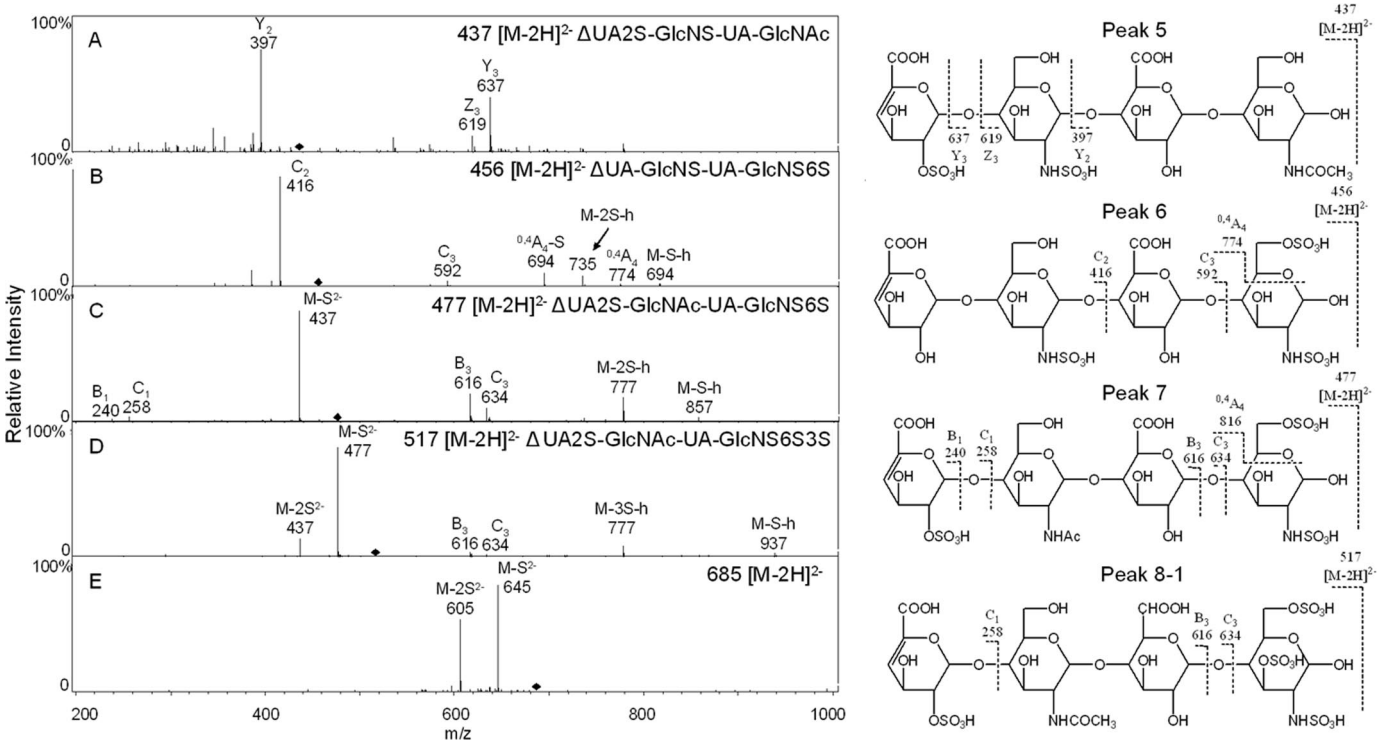

FIGURE 6. **Structure determination of hFF aHS and iHS tetrasaccharides by MS/MS.** Shown are representative MS/MS spectra (*left*) and deduced structures of aHS and iHS tetrasaccharides. *A*, glycosidic bond cleavage fragment ions (Y_2, Y_3, Z_3) identify peak 5 as ΔUA2S-GlcNS-UA-GlcNAc. *B*, glycosidic bond cleavage ions (C_2, C_3) and a cross-ring cleavage fragment ion ($^{0,4}A_4$) reveal *peak 6* as ΔUA-GlcNS-UA-GlcNS6S. *C*, glycosidic bond cleavage ions (B_1, C_1, B_3, C_3) and a cross-ring cleavage fragment ion ($^{0,4}A_4$) show *peak 7* to be ΔUA2S-GlcNAc-UA-GlcNS6S. *D*, glycosidic bond cleavage fragment ions (C_1, B_3, C_3) identify *peak 8-1* as ΔUA2S-GlcNAc-UA-GlcNS6S3S.; *E*, MS/MS spectrum of hexasaccharide in *peak 8-2*.

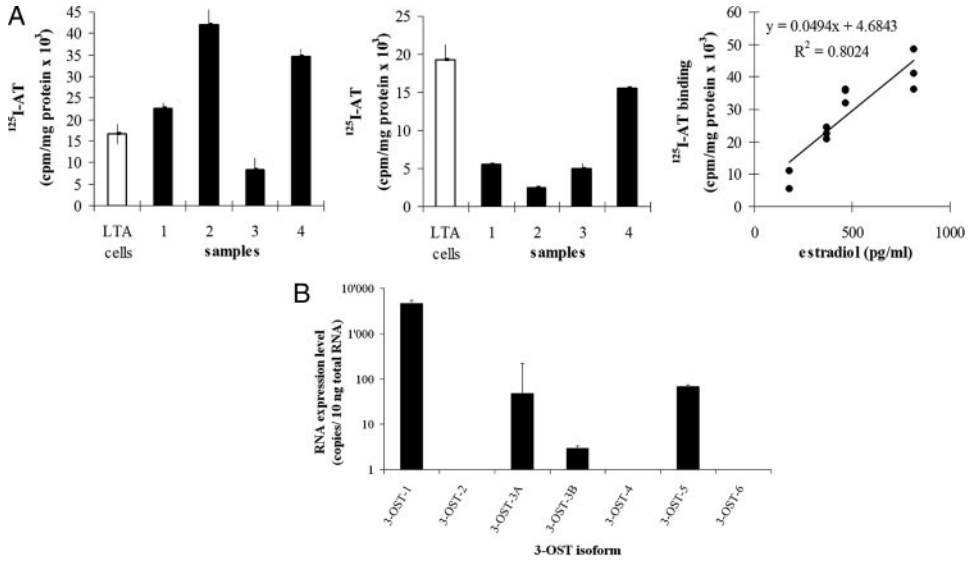

FIGURE 7. **aHSPG in human GC.** *A*, human GCs produce aHSPG. GCs from four different patients were cultured. Cell-bound and soluble aHSPG were detected by ^{125}I-AT cell binding assay (*left*) and ^{125}I-AT ligand-binding assay (*center*), respectively. The amount of aHSPG was variable in different patients but was comparable with the reference cell line LTA (*right*). The amount of cell-bound aHSPG was correlated to the estradiol secreted by the cells, reflecting the extent to the cells response to FSH. *B*, 3-*O*-sulfotransferase isoforms expression in human granulosa cells. 3-OST transcript copies per 10 ng of RNA. Mean values from five different patients are shown.

subsequent luteal phase, a procoagulant state exists. Within the remnant antral cavity, follicular fluid forms a fibrin clot that serves as a provisional matrix for the migration of luteal cells and for angiogenesis to support the formation of the corpus luteum (28). The results presented in this study provide compelling evidence that the anticoagulant state of preovulatory hFF involves the potent anticoagulant activity of aHSPGs synthesized by GCs. We additionally find that the iHSPGs from GCs produce an unusually high content of 3-*O*-sulfated residues, which suggests this unique HS form may exhibit an unanticipated novel function.

Anticoagulant Role of aHSPGs from GCs—GC synthesis of aHSPGs exhibits several features that suggest aHSPGs may play a key role in the anticoagulant state of preovulatory hFF. First, we found that human GCs strongly express transcripts for 3-OST-1, which is the major biologic source of aHS (3). Human GCs additionally express about 100-fold lower levels of 3-OST-$3_{A/B}$ and 3-OST-5, which are less efficient at producing aHS than 3-OST-1 (7, 20, 29). Second, cultured rat (12) and human GCs secrete aHSPGs, which would enable accumulation of these molecules in follicular fluid. Third, aHSPG production varies with follicle development. In the rat ovary, we have previously shown that aHSPG levels peak in pre-ovulatory GCs, which reflect the ability of rat GCs to synthesize and secrete aHSPGs in response to FSH stimulation (9, 10, 12). Similarly, we have now found that for cultured human GCs there is a tight correlation between aHSPG production and estradiol output. Thus, maximal levels of aHSPGs should occur in ovulatory follicular fluid, which requires maximal anticoagulant tone.

The fluidity of hFF likely stems from multiple factors. Compared with plasma, hFF contains high levels of tissue factor pathway inhibitor, which may limit initiation of coagulation (15). Similarly, hFF contains low concentrations of Factors V and VIII (15, 31), which might limit amplification of thrombin formation (32). In addition, hFF contains AT levels that are comparable with plasma. AT is able to inhibit virtually all coagulation proteases, so there is a potential for hFF to exhibit a strong anticoagulant tone. Indeed, we found that native hFF contains an AT-dependent "heparin-like" factor with an anti-Factor Xa activity of 2.5 IU/ml. This activity is 2.5–5-fold higher than the therapeutic range for heparin anticoagulation, suggesting that it could be a physiologically significant inhibitor of fibrin deposition in the ovary. This heparin-like activity was found to be due to the presence of exceptionally high levels of aHSPGs; their levels correlate to the anti-Factor Xa activity in hFF.

Purification of hFF aHS revealed several unusual features. First, aHS chains included 50.4% of total HS from hFF. To the best of our knowledge, this is the highest aHS content of HS derived from a natural source. The highest levels of aHS previously described were found in Reichert's membrane HS (33) and mast cell heparin, where only about 30% of HS chains are aHS. Moreover, aHS content is typically much lower (*e.g.* 6% of rat granulosa cell HS; 1–10% of endothelial cell HS) (12, 34, 35). Second, pure aHS has an extremely high anti-Factor Xa-specific activity of 167 IU/mg,[5] which is comparable with that of unfractionated heparin. Third, aHS is greatly enriched in 3-*O*-sulfated residues, which are essential for AT binding. The one-dimensional ^{1}H NMR analysis showed that aHS contains greater 3-*O*-sulfated glucosamine residues than iHS. These residues are normally extremely rare and were not detected in the one-dimensional ^{1}H NMR spectra of HS from human liver (36), mouse lung, and mouse kidney (37). HPLC-MS followed by MS/MS analysis revealed that 11.7% of aHS is a heparin lyase-resistant tetrasaccharide containing GlcNS6S**3S**. Because aHS contains more 3-*O*-sulfates than iHS, it is likely that additional 3-*O*-sulfates occur within the heparin lyase-resistant hexasaccharide that is 10-fold more abundant in aHS than iHS. Combined, these highly unusual structural features indicate that the HS biosynthetic machinery of follicular phase granulosa cells is uniquely tuned for extensive production of aHS. The relevance of this pathway is highlighted by the aHSPG-deficient *Hs3st1*$^{-/-}$ mice, which have strongly decreased fertility (11).[6]

Subsequent to ovulation, dramatic alterations must occur in the luteal phase, when follicular fluid undergoes clotting. Upon the transition into the luteal phase, there is a dramatic reduc-

[5] We have used this specific activity to calibrate the amounts of aHSPG detected by the ^{125}I-AT-ligand binding assay. We determined that 1 μg of aHS binds 8.5 $\pm$ 2.5 $\times$ 10^6 cpm of ^{125}I-AT (supplemental Table 3). With this factor, we can now directly quantitate aHS levels in native hFF and could extend this approach to other biologic fluids.

[6] A. I. de Agostini, unpublished observations.

tion in aHS synthesis by GCs. Presumably there must also be a mechanism to "neutralize" the high levels of aHS that already accumulated in the follicular fluid. One potential mechanism could be degradation by heparanase, which is expressed in the luteinized granulosa, the theca interna of mature antral follicles, and in the corpus luteum (38). We note that recombinant heparanase has been shown to spare AT-binding sites in heparin (39). However, cleavage is only inhibited when 3-*O*-sulfates occur in a highly sulfated chain region (40) Our structural analyses clearly shows that GC aHS has a much lower sulfation level than heparin, so heparanase may well be able to cleave AT-binding sites in GC aHS.

A Role for iHS?—We found that hFF iHS does not contain AT-binding sites and yet has unusually high levels of 3-*O*-sulfated residues; levels were at least 10-fold higher than iHS isolated from other sources (12, 30, 41). Such a highly unusual composition suggests that hFF may mediate an unexpected function in the female reproductive tract, possibly in tissue remodeling and inflammation occurring in reproduction. This function could be manifest in the corpus luteum or within the uterus, possibly to modulate oocyte transport or embryonic implantation. Because GCs express multiple 3-OSTs, it will be important to analyze follicular fluid HS from *Hs3st1*$^{-/-}$ mice to determine whether there is an alteration in 3-*O*-sulfation of iHS.

Altogether, the abundance of 3-*O*-sulfated residues on aHS and iHS is inspiring for further analysis of pathophysiological function of these GAGs, and further work is underway in our laboratory to address these issues.

Acknowledgments—We are grateful to Jian Liu who has generously given us recombinant heparin lyases. We acknowledge the contribution of Didier Chardonnens, Dominique de Ziegler, and Taher El Barbary for the hFF collection and of Jacqueline Fournier, Raynald Luthi, and Virna Laplana for the preparation of native hFF. We thank Paul Bischof for the determination of estradiol in hFF samples and Yann Burnel for performing coagulation assays.

REFERENCES

1. Rosenberg, R. D., Shworak, N. W., Liu, J., Schwartz, J. J., and Zhang, L. (1997) *J. Clin. Investig.* **99,** 2062–2070
2. Carrell, R., Skinner, R., Jin, L., and Abrahams, J. P. (1997) *Thromb. Haemostasis* **78,** 516–519
3. HajMohammadi, S., Enjoyji, K., Princivalle, M., Christi, P., Lech, M., Beeler, D., Rayburn, H., Schwartz, J. J., Barzagar, S., de Agostini, A. I., Post, M. J., Rosenberg, R. D., and Shworak, N. W. (2003) *J. Clin. Investig.* **111,** 989–999
4. Shworak, N. W., Liu, J., Petros, L. M., Zhang, L., Kobayashi, M., Copeland, N. G., Jenkins, N. A., and Rosenberg, R. D. (1999) *J. Biol. Chem.* **274,** 5170–5184
5. Liu, J., Shworak, N. W., Sinay, P., Schwartz, J. J., Zhang, L., Fritze, L. M., and Rosenberg, R. D. (1999) *J. Biol. Chem.* **274,** 5185–5192
6. Liu, J., Shriver, Z., Blaiklock, P., Yoshida, K., Sasisekharan, R., and Rosenberg, R. D. (1999) *J. Biol. Chem.* **274,** 38155–38162
7. Xia, G., Chen, J., Tiwari, V., Ju, W., Li, J. P., Malmstrom, A., Shukla, D., and Liu, J. (2002) *J. Biol. Chem.* **277,** 37912–37919
8. Ye, S., Luo, Y., Lu, W., Jones, R. B., Linhardt, R. J., Capila, I., Toida, T., Kan, M., Pelletier, H., and McKeehan, W. L. (2001) *Biochemistry* **40,** 14429–14439
9. Princivalle, M., Hasan, S., Hosseini, G., and de Agostini, A. I. (2001) *Glycobiology* **11,** 183–194
10. Hasan, S., Hosseini, G., Princivalle, M., Dong, J. C., Birsan, D., Cagide, C., and de Agostini, A. I. (2002) *Biol. Reprod.* **66,** 144–158
11. de Agostini, A. I. (2006) *Swiss Med. Wkly.* **136,** 583–590
12. Hosseini, G., Liu, J., and de Agostini, A. (1996) *J. Biol. Chem.* **271,** 22090–22099
13. de Agostini, A. I., Ramus, M. A., and Rosenberg, R. D. (1994) *J. Cell. Biochem.* **54,** 174–185
14. Roach, L. E., Petrik, J. J., Plante, L., LaMarre, J., and Gentry, P. A. (2002) *Biol. Reprod.* **66,** 1350–1358
15. Shimada, H., Kasakura, S., Shiotani, M., Nakamura, K., Ikeuchi, M., Hoshino, T., Komatsu, T., Ihara, Y., Sohma, M., Maeda, Y., Matsuura, R., Nakamura, S., Hine, C., Ohkura, N., and Kato, H. (2001) *Biol. Reprod.* **64,** 1739–1745
16. Bjornsson, S. (1998) *Anal. Biochem.* **256,** 229–237
17. Shworak, N. W., Shirakawa, M., Colliec-Jouault, S., Liu, J., Mulligan, R. C., Biriny, L. K., and Rosenberg, R. D. (1994) *J. Biol. Chem.* **269,** 24941–24952
18. England, B. G., Niswender, G. D., and Midgley, A. R. (1974) *J. Clin. Endocrinol. Metab.* **38,** 42–50
19. Lawrence, R., Yabe, T., HajMohammadi, S., Rhodes, J., McNeely, M., Liu, J., Lamperti, E. D., Toselli, P. A., Lech, M., Spear, P. G., Rosenberg, R. D., and Shworak, N. W. (2007) *Matrix Biol.* **26,** 442–455
20. Girardin, E. P., HajMohammadi, S., Birmele, B., Helisch, A., Shworak, N. W., and de Agostini, A. I. (2005) *J. Biol. Chem.* **280,** 38059–38070
21. Daniels, R. J., Peden, J. F., Lloyd, C., Horsley, S. W., Clark, K., Tufarelli, C., Kearney, L., Buckle, V. J., Doggett, N. A., Flint, J., and Higgs, D. R. (2001) *Hum. Mol. Genet.* **10,** 339–352
22. Therien, I., Bergeron, A., Bousquet, D., and Manjunath, P. (2005) *Mol. Reprod. Dev.* **71,** 97–106
23. McArthur, M. E., Irving-Rodgers, H. F., Byers, S., and Rodgers, R. J. (2000) *Biol. Reprod.* **63,** 913–924
24. Eriksen, G. V., Carlstedt, I., Morgelin, M., Uldbjerg, N., and Malmstrom, A. (1999) *Biochem. J.* **340,** 613–620
25. Eriksen, G. V., Malmstrom, A., and Uldbjerg, N. (1997) *Fertil. Steril.* **68,** 791–798
26. Zhang, L., Yoshida, K., Liu, J., and Rosenberg, R. D. (1999) *J. Biol. Chem.* **274,** 5681–5691
27. Shriver, Z., Sundaram, M., Venkataraman, G., Fareed, J., Linhardt, R., Biemann, K., and Sasisekharan, R. (2000) *Proc. Natl. Acad. Sci. U. S. A.* **97,** 10365–10370
28. Kamat, B. R., Brown, L. F., Manseau, E. J., Senger, D. R., and Dvorak, H. F. (1995) *Am. J. Pathol.* **146,** 157–165
29. Yabe, T., Shukla, D., Spear, P. G., Rosenberg, R. D., Seeberger, P. H., and Shworak, N. W. (2001) *Biochem. J.* **359,** 235–241
30. Shworak, N. W., Shirakawa, M., Mulligan, R. C., and Rosenberg, R. D. (1994) *J. Biol. Chem.* **269,** 21204–21214
31. Gentry, P. A., Plante, L., Schroeder, M. O., LaMarre, J., Young, J. E., and Dodds, W. G. (2000) *Fertil. Steril.* **73,** 848–854
32. Bungay, S. D., Gentry, P. A., and Gentry, R. D. (2006) *Bull. Math. Biol.* **68,** 2283–2302
33. Pejler, G., Backstrom, G., Lindahl, U., Paulsson, M., Dziadek, M., Fujiwara, S., and Timpl, R. (1987) *J. Biol. Chem.* **262,** 5036–5043
34. de Agostini, A. I., Watkins, S. C., Slayter, H. S., Youssoufian, H., and Rosenberg, R. D. (1990) *J. Cell Biol.* **111,** 1293–1304
35. Marcum, J. A., Atha, D. H., Fritze, L. M. S., Nawroth, P., Stern, D., and Rosenberg, R. D. (1986) *J. Biol. Chem.* **261,** 7507–7517
36. Vongchan, P., Warda, M., Toyoda, H., Toida, T., Marks, R. M., and Linhardt, R. J. (2005) *Biochim. Biophys. Acta* **1721,** 1–8
37. Warda, M., Toida, T., Zhang, F., Sun, P., Munoz, E., Xie, J., and Linhardt, R. J. (2006) *Glycoconj. J.* **23,** 555–563
38. Haimov-Kochman, R., Prus, D., Zcharia, E., Goldman-Wohl, D. S., Natanson-Yaron, S., Greenfield, C., Anteby, E. Y., Reich, R., Orly, J., Tsafriri, A., Hurwitz, A., Vlodavsky, I., and Yagel, S. (2005) *Biol. Reprod.* **73,** 20–28
39. Gong, F., Jemth, P., Escobar Galvis, M. L., Vlodavsky, I., Horner, A., Lindahl, U., and Li, J. P. (2003) *J. Biol. Chem.* **278,** 35152–35158
40. Okada, Y., Yamada, S., Toyoshima, M., Dong, J., Nakajima, M., and Sugahara, K. (2002) *J. Biol. Chem.* **277,** 42488–42495
41. Kojima, T., Leone, C. W., Marchildon, G. A., Marcum, J. A., and Rosenberg, R. D. (1992) *J. Biol. Chem.* **267,** 4859–4869